

Generalized Gibbs Ensemble for Heisenberg Spin Chains

Balázs Pozsgay¹

¹MTA-BME "Momentum" Statistical Field Theory Research Group
1111 Budapest, Budafoki út 8, Hungary

November 27, 2024

Abstract

We consider the Generalized Gibbs Ensemble (GGE) in the context of global quantum quenches in XXZ Heisenberg spin chains. Embedding the GGE into the Quantum Transfer Matrix formalism we develop an iterative procedure to fix the Lagrange-multipliers and to calculate predictions for the long-time limit of short-range correlators. The main idea is to consider truncated GGE's with only a finite number of charges and to investigate the convergence of the numerical results as the truncation level is increased. As an example we consider a quantum quench situation where the system is initially prepared in the Néel state and then evolves with an XXZ Hamiltonian with anisotropy $\Delta > 1$. We provide predictions for short range correlators and gather numerical evidence that the iterative procedure indeed converges. The results show that the system retains memory of the initial condition, and there are clear differences between the numerical values of the correlators as calculated from the purely thermal and the Generalized Gibbs ensembles.

1 Introduction

Thermalization is a physical process whereby an isolated system reaches thermal equilibrium through the interactions of its constituents. Energy is conserved by time evolution, therefore the temperature of the equilibrated system is determined solely by the available energy at the beginning of the relaxation process.

In quantum mechanics time evolution is represented by a unitary operation on the Hilbert space. When at $t = 0$ the system is in a state Ψ_0 , the density matrix evolves according to

$$\rho(t) = |\Psi(t)\rangle\langle\Psi(t)| = e^{-iHt}|\Psi_0\rangle\langle\Psi_0|e^{iHt}$$

Therefore, the density matrix itself never thermalizes. Instead, thermalization in quantum mechanics means that the expectation values of physical observables (or equivalently the matrix elements of the reduced density matrices) assume values which are equal to those calculated in a thermal ensemble. In a generic quantum mechanical system this is expected to happen, if there are no external driving forces present [1, 2].

The situation is different in the case of integrable models, in which there exists an infinite family of mutually commuting quantum charges such that the Hamiltonian is a member of the infinite series:

$$[Q_j, Q_k] = 0 \quad \text{for } j, k = 1 \dots \infty, \quad Q_2 \sim H \tag{1.1}$$

It follows that time evolution conserves the expectation values of all charges, which prevents thermalization in the usual sense. Instead, relaxation to a Generalized Gibbs Ensemble (GGE) was proposed in [3]. The main idea is to construct a thermodynamic ensemble where the statistical weights depend also on all the higher charges and not only on the energy. It was proposed that the long-time limit of quantum observables after a quantum quench should be described by a GGE with appropriately chosen Lagrange multipliers for the individual charges.

A huge amount of work was dedicated to study global quantum quenches in integrable models (see [4, 5] and references therein). Most of the available results concern theories equivalent to free fermions [6, 7, 8, 9, 10, 11, 12, 13] or interacting models in the CFT limit [14]. One of the most important goals

is to determine whether the GGE provides a valid description of the possible steady states arising in non-equilibrium situations. In the case of free theories the answer seems to be a general affirmative yes [15, 9, 13, 16, 17, 18, 19, 20, 21], whereas the question is still unresolved for genuinely interacting theories. A further open problem in interacting theories is how to use the GGE to make actual predictions for physical observables.

In Bethe Ansatz solvable models with only a single particle type the GGE hypothesis leads to a generalization of the Thermodynamic Bethe Ansatz (TBA) framework [22, 23]. Originally the TBA was developed to treat the purely thermal case [24, 25], but the addition of the higher charges does not modify its essential properties [23]. In principle the generalized TBA (or GTBA) encodes all thermodynamic properties and it can give predictions for the correlation functions as well [26, 27, 28]. In the Lieb-Liniger model studied in [22, 23, 4], however, this can not be carried out because the construction of the higher charges seems to be an insurmountable problem [29] and therefore the Lagrange multipliers entering the GGE can not be fixed. Instead, information about the overlaps between pre-quench and post-quench states was used in [22] to set up the GGE.

It is a very natural idea to apply the GTBA formalism to XXZ spin chains, where all higher charges can be constructed using their definition via the transfer matrix, or alternatively with the help of the boost operator [30, 31]. However, the infinite family of particle types (the strings of different length) lead to an infinite set of GTBA equations. Although it has been demonstrated that even such an infinite set can be treated numerically [32], fixing the Lagrange multipliers for the GGE through TBA seems extremely difficult.

An alternative to the TBA is the Quantum Transfer Matrix (QTM) method [33, 34], which leads to a single non-linear integral equation replacing the infinite set of the TBA [35]. Moreover, there are very efficient methods available to compute short-range correlations with the QTM [36, 37, 38]. The simplicity of the QTM with respect to the TBA makes it an excellent candidate to describe the GGE. The idea of adding higher charges to the QTM is not new: it was used in [39, 40] to calculate thermal conductivities and in [41, 42] to study the phase diagram and thermal properties of integrable spin chains with competing interactions.

In the present paper we apply the QTM formalism to set up the GGE for the spin chains. As an application we consider a specific example of a global quench, namely time evolution starting from the Néel state (in terms of the anisotropy Δ , this corresponds to a quench from $\Delta = \infty$ to finite Δ). Although the relaxation of the antiferromagnetic order was already studied by different methods in [43, 5], these works did not consider the long-time limit of correlation functions.

The paper is organized as follows. In Section 2 we pose the problem in general terms and explain our procedure to obtain the GGE as a limit of truncated GGE's. In Section 3 we present the extension of the QTM method to include a finite number of higher charges. Section 4 includes calculations concerning the explicit form of the conserved charges and their mean values in the Néel state. In Section 5 we present our numerical results and finally we conclude in Section 6.

2 Global quenches in integrable models

Consider a 1D lattice model of L sites with periodic boundary conditions. The local spin variables are σ_j with $j = 1 \dots L$ and they can take K values, therefore the Hilbert-space of the system is

$$\mathcal{H} = \otimes^L (\mathbb{C}^K).$$

Consider a family of Hamiltonians of the form

$$H = \sum_{j=1}^L u_j + h_{j,j+1}, \tag{2.1}$$

where it is understood that u_j and $h_{j,j+1}$ are given by a translation of one-site and two site-operators u_1 and $h_{1,2}$ which might depend on a finite set of coupling constants. The generalization to Hamiltonians with multi-site interactions is straightforward. Note that in (2.1) periodic boundary conditions are assumed.

In this work we consider the situation of a sudden global quench. At $t = 0$ we prepare the system in a state $|\Psi(t=0)\rangle = |\Psi_0\rangle$ which might be the ground state of a Hamiltonian H_0 or a state prepared according to a well-defined rule. In the latter case we only require that $|\Psi_0\rangle$ be defined in a natural way for any L or at least any even L .

At $t = 0$ we change the parameters of the system such that time evolution for $t > 0$ will be governed by the post-quench Hamiltonian H :

$$|\Psi(t)\rangle = e^{-iHt}|\Psi_0\rangle.$$

Consider a localized quantum observable \mathcal{O} . In the examples to be investigated below \mathcal{O} will be a correlation function of local spin operators on neighboring sites or only a few sites apart. The time dependence of this observable is

$$\mathcal{O}(L, t) = \langle \Psi(t) | \mathcal{O} | \Psi(t) \rangle = \langle \Psi_0 | e^{iHt} \mathcal{O} e^{-iHt} | \Psi_0 \rangle.$$

In the formulas above it was understood that all quantities depend on the volume L . We will be interested in the thermodynamic limit:

$$\mathcal{O}(t) = \lim_{L \rightarrow \infty} \mathcal{O}(L, t).$$

Moreover we consider the infinite time limit of the observable:

$$\bar{\mathcal{O}} = \lim_{t \rightarrow \infty} \mathcal{O}(t). \quad (2.2)$$

In a generic non-integrable system we expect the phenomenon of thermalization. This means that all long-time averages are described by a thermal ensemble with an effective temperature $T = 1/\beta$:

$$\bar{\mathcal{O}} = \frac{1}{Z} \text{Tr} (\mathcal{O} e^{-\beta H}) \quad Z = \text{Tr} e^{-\beta H}. \quad (2.3)$$

Time evolution conserves the expectation value for the energy, therefore the Lagrange multiplier β can be fixed (at least in principle) by the requirement

$$\langle H \rangle = -\frac{d}{d\beta} \log Z = \langle \Psi_0 | H | \Psi_0 \rangle. \quad (2.4)$$

A central statement of thermalization is that there is a single effective temperature T for *all* quantum observables. Note that in formulas (2.3)-(2.4) an implicit infinite volume limit is understood.

The situation is expected to be different when H is integrable, in which case the thermalization hypothesis does not hold. The reason for this is the following. In integrable models there exists an infinite set of conserved charges Q_j , $j = 1 \dots \infty$ which commute among themselves:

$$[Q_j, Q_k] = 0. \quad (2.5)$$

The Hamiltonian is a member of the series, typically $H \sim Q_2$ (the first charge Q_1 is usually the momentum operator). It follows from (2.5) that the expectation values of all the charges are conserved in time. The Q_j are constructed as sums of localized operators, therefore (2.3) should apply if the system thermalizes. However, the thermal ensemble would typically yield mean values for the conserved charges which differ from those measured in the initial state, therefore (2.3) can not be valid and thermalization can not occur.

To describe the long-time average of observables in integrable models the Generalized Gibbs Ensemble (GGE) was proposed in [3]. Setting aside convergence properties for a moment the hypothesis of GGE can be formulated as follows: There exists a set of couplings $\{\beta_j\}$ such that the long-time stationary state of the system is described by the density matrix

$$\rho_{GGE} = \frac{1}{Z_{GGE}} \exp \left(- \sum_{j=1}^{\infty} \beta_j Q_j \right) \quad Z_{GGE} = \text{Tr} \exp \left(- \sum_{j=1}^{\infty} \beta_j Q_j \right). \quad (2.6)$$

Physical quantities in this ensemble are given by

$$\mathcal{O}_{GGE} = \text{Tr} (\mathcal{O} \rho_{GGE}). \quad (2.7)$$

Expectation values of the charges are conserved in time, therefore the Lagrange multipliers can be fixed (at least in principle) by requiring

$$\langle Q_j \rangle = -\frac{d}{d\beta_j} \log Z_{GGE} = \langle \Psi_0 | Q_j | \Psi_0 \rangle, \quad j = 1 \dots \infty. \quad (2.8)$$

The GGE hypothesis states that for any localized operator the expectation value obtained by the equations (2.6)-(2.8) is equal to the long-time average:

$$\mathcal{O}_{GGE} = \bar{\mathcal{O}}. \quad (2.9)$$

Again, a crucial statement is that there is a single set of β_j which determines *all* physical observables. Note that all conserved charges need to be added to (2.6), otherwise the GGE can not be complete.

Equations (2.6)-(2.8) completely specify the GGE. However, in practice it is impossible to fix all the β_j and the convergence of the infinite sum is also not guaranteed. In this work we propose to obtain the GGE as a limit of an iterative procedure, where at step k we only consider the first k charges. This idea also appeared in the very recent paper [13] which concerned the quantum Ising chain.

To be specific, we define sets of parameters $\{\beta_j^{(k)}, j = 1 \dots k\}$ which generate the density matrices of truncated GGE's:

$$\rho^{(k)} = \frac{1}{Z^{(k)}} \exp \left(- \sum_{j=1}^k \beta_j^{(k)} Q_j \right) \quad Z^{(k)} = \text{Tr} \exp \left(- \sum_{j=1}^k \beta_j^{(k)} Q_j \right). \quad (2.10)$$

We call the number k the truncation level. The $\beta_j^{(k)}$ are chosen such that

$$-\frac{d}{d\beta_j} \log Z^{(k)} = \langle \Psi_0 | Q_j | \Psi_0 \rangle, \quad j = 1 \dots k. \quad (2.11)$$

For the quantum observables we obtain a series

$$\mathcal{O}^{(k)} = \text{Tr} (\mathcal{O} \rho^{(k)}). \quad (2.12)$$

The actual GGE average is then given by the limit

$$\mathcal{O}_{GGE} = \lim_{k \rightarrow \infty} \mathcal{O}^{(k)}. \quad (2.13)$$

This procedure provides a well-defined recipe to obtain the GGE averages, but we are faced with the following questions: Does the limit (2.13) exist? Does it exist for all localized physical observables or maybe even non-local quantities like correlation lengths? How do the convergence properties depend on the Hamiltonian and the initial state?

While we can not answer these questions in their full generality, we will present one non-trivial example in XXZ spin chains where numerical evidence shows that the limit (2.13) exists for short-range correlation functions. This way the GGE indeed gives predictions which could be compared to experiments or independent numerical calculations.

3 Thermal and Generalized Gibbs ensembles for the XXZ spin chain

In this work we consider quantum quenches in spin-1/2 XXZ chains. The Hamiltonian is given by

$$H_{XXZ}(J, \Delta, h) = J \sum_{j=1}^L (\sigma_j^x \sigma_{j+1}^x + \sigma_j^y \sigma_{j+1}^y + \Delta (\sigma_j^z \sigma_{j+1}^z - 1)) + h \sum_{j=1}^L \sigma_j^z. \quad (3.1)$$

In the following we will only consider the zero-field case $h = 0$. Moreover we set $J = 1$ and restrict ourselves to the regime $\Delta > 0$.

In the present section we set up the general framework of the GGE, independent of the details of the initial state. Here we just assume that the mean values of the conserved charges can be calculated with exact methods. Details of how to do this will be provided in the next section, and we give a few comments about more general situations in the Conclusions.

The XXZ model is integrable for arbitrary Δ . Its spectrum is given by the Bethe Ansatz [44, 45, 46, 47] and the higher conserved charges can be constructed using the transfer matrix formalism.

Consider the R-matrix acting on $\mathbb{C}^2 \otimes \mathbb{C}^2$ given as

$$R(u) = \frac{1}{\sinh(u + \eta)} \begin{pmatrix} \sinh(u + \eta) & & & \\ & \sinh(u) & \sinh(\eta) & \\ & \sinh(\eta) & \sinh(u) & \\ & & & \sinh(u + \eta) \end{pmatrix}. \quad (3.2)$$

Here u is the spectral parameter and η is a complex number related to the anisotropy by $\Delta = \cosh \eta$.

The monodromy matrix is constructed as

$$T(u) = L_M(u) \dots L_1(u),$$

where $L_j(u)$ are local Lax-operators given by

$$L_j(u) = R_{0j}(u),$$

and the index 0 stands for the auxiliary spin space. In this space $T(u)$ can be written as

$$T(u) = \begin{pmatrix} A(u) & B(u) \\ C(u) & D(u) \end{pmatrix},$$

where $A(u), B(u), C(u), D(u)$ are operators acting on the spin chain.

The transfer matrix is given by the trace

$$\tau(u) = \text{Tr}_0 T(u) = A(u) + D(u).$$

The R -matrix satisfies the Yang-Baxter equation [48, 49] which leads to the commutativity of the transfer matrices:

$$[\tau(u), \tau(v)] = 0.$$

This property is used to define the conserved charges of the model. It can be shown that

$$\tau(0) = U,$$

with U being the translation operator on the chain and it can be considered as the first conserved charge: $U = e^{iQ_1}$, where Q_1 is the momentum operator. The other charges are defined as logarithmic derivatives of the transfer matrix at $u = 0$:

$$Q_j = \left(\frac{d}{du} \right)^{j-1} \log \tau(u). \quad (3.3)$$

It was shown in [50] that the Q_j defined this way are local in the sense that they are given as sums of products of spin variables such that they only span a finite segment of the chain of length j . We note that using the normalizations above the second conserved charge is

$$Q_2 = \frac{1}{2 \sinh \eta} H_{XXZ}.$$

Eigenstates of the commuting family of transfer matrices can be constructed using the Algebraic Bethe Ansatz [51]. We choose the reference state $|F\rangle$ to be the ferromagnetic state with all spins up. Bethe states are then constructed by acting with the B -operators:

$$|\mu_1, \dots, \mu_M\rangle = \prod_{j=1}^M B(\mu_j) |F\rangle. \quad (3.4)$$

Here the complex variables μ_j are the rapidities of the interacting spin waves. Such a state is an eigenstate of the family of commuting transfer matrices if the Bethe equations are satisfied:

$$d(\mu_j) \prod_{k \neq j} \frac{\sinh(\mu_j - \mu_k + \eta)}{\sinh(\mu_j - \mu_k - \eta)} = 1, \quad (3.5)$$

where

$$d(u) = \langle F | D(u) | F \rangle = \left(\frac{\sinh(u)}{\sinh(u + \eta)} \right)^L. \quad (3.6)$$

It can be shown that the states (3.4) are identical to the states constructed by the coordinate Bethe Ansatz.

In the regime $\Delta > 1$ we have $\eta \in \mathbb{R}$ and the usual one-string solutions of the Bethe equations are of the form $\mu = i\lambda - \eta/2$ with $\lambda \in \mathbb{R}$. On the other hand, when $\Delta < 1$ we have $\eta = i\gamma$ with $\gamma \in \mathbb{R}$ and the usual one-string solutions are $\mu = \lambda - i\gamma/2$ with $\lambda \in \mathbb{R}$. The isotropic case ($\Delta = 1$) can be obtained by a limiting procedure, but we do not consider this here.

In the following we will need the eigenvalues of the conserved charges on the Bethe states. The Algebraic Bethe Ansatz yields the following transfer matrix eigenvalue:

$$t(u, \{\mu\}_M) = \prod_{j=1}^M \frac{\sinh(u - \mu_j - \eta)}{\sinh(u - \mu_j)} + d(u) \prod_{j=1}^M \frac{\sinh(u - \mu_j + \eta)}{\sinh(u - \mu_j)}.$$

Taking the logarithmic derivative gives

$$Q_j |\mu_1, \dots, \mu_N\rangle = \left(\sum_{k=1}^N q_j(\mu_k) \right) |\mu_1, \dots, \mu_N\rangle$$

with

$$q_j(\mu) = \left. \left(\left(\frac{\partial}{\partial u} \right)^{j-1} \log \frac{\sinh(u - \mu - \eta)}{\sinh(u - \mu)} \right) \right|_{u=0}. \quad (3.7)$$

Here we assumed that $L > j$ such that the terms originating from $d(u)$ are all zero.

For the second charge (proportional to the one-string energy) we obtain

$$q_2(\mu) = \frac{\cosh(\mu)}{\sinh(\mu)} - \frac{\cosh(\mu + \eta)}{\sinh(\mu + \eta)}.$$

The formulas for the higher charges can be written in the form

$$q_j(\mu) = G_j(x_0) - G_j(x_+), \quad (3.8)$$

where

$$x_0 = \frac{\cosh(\mu)}{\sinh(\mu)} \quad x_+ = \frac{\cosh(\mu + \eta)}{\sinh(\mu + \eta)}$$

and the $G_j(x)$ are polynomials satisfying the recursion

$$G_{j+1}(x) = (x^2 - 1) \frac{d}{dx} G_j(x), \quad G_2(x) = x. \quad (3.9)$$

Thermal ensembles for the XXZ spin chains can be constructed using the so-called Quantum Transfer Matrix (QTM) formalism [33, 34]. The goal is to construct the density matrix

$$\rho = \frac{1}{Z} \exp(-\beta Q_2) \quad Z = \text{Tr} \exp(-\beta Q_2).$$

The central idea is to write down the Trotter-Suzuki decomposition of $\exp(-\beta Q_2)$:

$$\exp(-\beta Q_2) \approx \left(1 - \frac{\beta}{N} Q_2 \right)^N \approx (\tau^{-1}(0) \tau(-\beta/N))^N. \quad (3.10)$$

Here N is called the Trotter number and the two relations above become equalities in the $N \rightarrow \infty$ limit. At finite N the trace

$$Z_{N,L} = \text{Tr} (\tau^{-1}(0) \tau(-\beta/N))^N$$

can be interpreted as a partition function of a six-vertex model with L vertical and N horizontal lines. The vertical lines correspond to the original spin spaces and the horizontal ones are auxiliary spaces. The partition function can be obtained alternatively by "quantizing" the system in the horizontal direction introducing the "Quantum Transfer Matrix" which acts on the auxiliary spaces. The $L \rightarrow \infty$ limit of the partition function can then be obtained by the largest eigenvalue of the QTM. It is known that the QTM is gapped in the sense that the second largest eigenvalue is separated from the largest by a finite distance

even in the $N \rightarrow \infty$ limit. This means that all thermodynamic properties will be determined by the single leading eigenstate of the QTM. This state can be found by the Algebraic Bethe Ansatz and its transfer matrix eigenvalues can be computed both at finite N and in the Trotter limit. For the details of this procedure we refer the reader to the review [34].

In the Trotter limit the partition function can be expressed as

$$\log Z = -fL + \dots,$$

where the dots denote exponentially small corrections in L and the free energy density is given by

$$f = - \int_C \frac{d\omega}{2\pi i} \frac{\sinh \eta \log(1 + \mathbf{a}(\omega))}{\sinh \omega \sinh(\omega + \eta)}. \quad (3.11)$$

Here $\mathbf{a}(\lambda)$ is an auxiliary function defined on the complex plane which satisfies the nonlinear integral equation (NLIE)

$$\log \mathbf{a}(\lambda) = -\beta q_2(\lambda) - \int_C \frac{d\omega}{2\pi i} \frac{\sinh 2\eta \log(1 + \mathbf{a}(\omega))}{\sinh(\lambda - \omega + \eta) \sinh(\lambda - \omega - \eta)}. \quad (3.12)$$

The contour C in the equations above depends on Δ . For the $\Delta > 1$ regime considered in the present work it can be chosen as a union of two straight line segments:

$$C = [-i\pi/2 + \alpha, i\pi/2 - \alpha] \cup [i\pi/2 - \alpha, -i\pi/2 + \alpha],$$

where $\alpha < \eta/2$ is an arbitrary parameter¹. Note that the first line segment runs upwards and the second runs downwards.

Thermodynamic properties of the spin chain can be calculated by taking derivatives of the free energy with respect to the physical parameters. Correlation functions are also accessible to this method. In [52] multiple integral formulas were calculated for the localized correlation functions. These were later found to factorize, ie. they can be expressed as sums of products of simple integrals [53] so that numerical results can be produced in a very efficient way [36, 37, 38].

It is a very natural idea to use the Trotter-Suzuki decomposition to construct the truncated GGE density matrices (2.10). In fact this method was already worked out in [39] where it was used to obtain thermal conductivities.

The main idea is that for any finite k the decomposition

$$\exp\left(-\sum_{j=2}^k \beta_j Q_j\right) \approx \left(1 - \frac{\sum_{j=2}^k \beta_j Q_j}{N} + o(1/N)\right)^N \quad (3.13)$$

holds. The right hand side can be obtained as

$$1 - \frac{\sum_{j=2}^k \beta_j Q_j}{N} = (\tau^{-1}(0))^{k-1} \tau(u_1) \tau(u_2) \dots \tau(u_{k-1}) + o(1/N), \quad (3.14)$$

with some appropriately chosen numbers u_j . For example in the case of $k = 3$ and non-zero β_3 a solution is

$$u_1 = \sqrt{\frac{\beta_3}{N}} - \frac{\beta_2}{2N} \quad u_2 = -\sqrt{\frac{\beta_3}{N}} - \frac{\beta_2}{2N}.$$

Assuming that the numbers u_j are found the partition function can be expressed as

$$Z_{N,L,k} = \text{Tr} \left[(\tau^{-1}(0))^{k-1} \tau(u_1) \tau(u_2) \dots \tau(u_{k-1}) \right]^N. \quad (3.15)$$

This is equivalent to a partition function of a six-vertex model, which can be quantized in the horizontal direction, leading to a modification of the original thermal QTM with a different set of inhomogeneities. We can assume that the analyticity properties necessary for the construction of the Trotter limit hold also in the modified problem, at least in a small neighborhood of the purely thermal case. Then the Trotter limit can be taken and it leads to

$$\log Z_{L,k} = -f^{(k)}L + \dots \quad (3.16)$$

¹When a magnetic field is added, α has to be large enough such that the contour encircles all Bethe roots of the QTM.

with

$$f^{(k)} = - \int_C \frac{d\omega}{2\pi i} \frac{\sinh \eta \log(1 + \mathbf{a}^{(k)}(\omega))}{\sinh \omega \sinh(\omega + \eta)}. \quad (3.17)$$

Here $\mathbf{a}^{(k)}$ is the auxiliary function solving the modified NLIE

$$\log \mathbf{a}^{(k)}(\lambda) = - \sum_{j=2}^k \beta_j q_j(\lambda) - \int_C \frac{d\omega}{2\pi i} \frac{\sinh 2\eta \log(1 + \mathbf{a}^{(k)}(\omega))}{\sinh(\lambda - \omega + \eta) \sinh(\lambda - \omega - \eta)}. \quad (3.18)$$

Note that the structure of the source term reflects the form of the truncated GGE density matrix (3.13).

Expectation values of conserved charges in the truncated GGE can be obtained by

$$\langle Q_j \rangle = L \frac{d}{d\beta_j} f^{(k)}. \quad (3.19)$$

Instead of taking the derivative of the formula (3.17) it is useful to express $f^{(k)}$ with the functions $\bar{\mathbf{a}}^{(k)} = 1/\mathbf{a}^{(k)}$. It can be shown that they satisfy

$$\log \bar{\mathbf{a}}^{(k)}(\lambda) = - \sum_{j=2}^k \beta_j q_j^-(\lambda) + \int_C \frac{d\omega}{2\pi i} \frac{\sinh 2\eta \log(1 + \bar{\mathbf{a}}^{(k)}(\omega))}{\sinh(\lambda - \omega + \eta) \sinh(\lambda - \omega - \eta)} \quad (3.20)$$

with

$$q_j^-(\mu) = G_j(x_0) - G_j(x_-), \quad (3.21)$$

where

$$x_0 = \frac{\cosh(\mu)}{\sinh(\mu)} \quad x_- = \frac{\cosh(\mu - \eta)}{\sinh(\mu - \eta)}.$$

The polynomials G_j are defined by (3.9). The free energy can be expressed with $\bar{\mathbf{a}}^{(k)}$ as

$$f^{(k)} = \int_C \frac{d\omega}{2\pi i} \frac{\sinh \eta \log(1 + \bar{\mathbf{a}}^{(k)}(\omega))}{\sinh \omega \sinh(\omega - \eta)}. \quad (3.22)$$

Taking the derivative of (3.20) and (3.22) with respect to β_j we introduce the functions

$$\mathbf{a}_j^{(k)}(\lambda) = - \frac{1}{\bar{\mathbf{a}}^{(k)}(\lambda)} \frac{\partial \bar{\mathbf{a}}^{(k)}(\lambda)}{\partial \beta_j} = \frac{1}{\bar{\mathbf{a}}^{(k)}(\lambda)} \frac{\partial \bar{\mathbf{a}}^{(k)}(\lambda)}{\partial \beta_j}.$$

They satisfy the linear equations

$$\mathbf{a}_j^{(k)}(\lambda) = - q_j^-(\lambda) + \int_C \frac{d\omega}{2\pi i} \frac{\sinh 2\eta}{\sinh(\lambda - \omega + \eta) \sinh(\lambda - \omega - \eta)} \frac{\mathbf{a}_j^{(k)}(\omega)}{1 + \mathbf{a}^{(k)}(\omega)}. \quad (3.23)$$

Finally the conserved charges in the truncated GGE are given by

$$\langle Q_j \rangle = L \int_C \frac{d\omega}{2\pi i} \frac{\sinh \eta}{\sinh \omega \sinh(\omega - \eta)} \frac{\mathbf{a}_j^{(k)}(\omega)}{1 + \mathbf{a}^{(k)}(\omega)}. \quad (3.24)$$

With this we have finished the construction of the truncated GGE using the QTM formalism. The remaining task is to calculate correlation functions in the truncated GGE.

In the derivation of the multiple integrals of [52] for the thermal correlations it is not necessary to know the exact position of the Bethe roots of the QTM; the only required information is that they can be surrounded by appropriate contours and that there exists an auxiliary function $\mathbf{a}(\lambda)$ which encodes the positions of the Bethe roots through the equation $\mathbf{a}(\lambda) = -1$ and which has a well-behaving Trotter limit. These conditions also hold for the truncated GGE's, at least in the neighborhood of a thermal case with a finite β_2 . In the multiple integrals of [52] the auxiliary function (or the combination $1/(1 + \mathbf{a}(\lambda))$) plays the role of a weight function, therefore the representation of [52] is valid also in the truncated GGE, provided that zeroes of $(1 + \mathbf{a}(\lambda))$ do not cross the contours. Based on continuity and symmetry arguments we expect that the Bethe roots will still be situated on the imaginary axis (when $\Delta > 1$) or the real axis (when $\Delta < 1$). Our numerical findings support this expectation in all cases we encountered (see Section

5). We conclude that the multiple integrals of [52] are also valid in the truncated GGE's, at least in the cases considered in the present work.

Factorized formulas for the correlators were developed in [53]. This factorization of the multiple integrals depends only on certain algebraic properties underlying the construction of correlation functions and not on the particular physical parameters (finite temperature or finite size) of the problem at hand [54, 38]. It follows that all the formulas already available for the thermal case are also valid in the truncated GGE, provided the calculations are carried out using the auxiliary functions $\alpha^{(k)}(\lambda)$ which satisfy (3.18) instead of (3.12). We refrain here from replicating the necessary formulas and refer the reader to the original papers [53, 38].

The method we described can be applied to construct the GGE within the QTM formalism and to calculate correlation functions in the GGE. The only input from the initial states is through the expectation values

$$\langle Q_j \rangle = \langle \Psi_0 | Q_j | \Psi_0 \rangle$$

which are used to fix the Lagrange multipliers. These mean values should be obtained exactly with use of explicit formulas for the Q_j or by other methods. In the next section we show one example where this task can be performed relatively easily.

4 Quench dynamics from the Néel state

We consider a quench with the Néel state as initial state:

$$|\Psi_0\rangle = |N\rangle = |+-+-+-+\dots\rangle.$$

This state is not translationally invariant, the correlation functions involving an odd number of spin operators (such as the magnetization $\langle \sigma_j^z \rangle$ itself) have an obvious position dependence. However, we expect that in the long time limit translational invariance of all correlation functions will be restored [43], in particular

$$\lim_{t \rightarrow \infty} \langle \sigma_j^z \rangle = 0.$$

We note that even though the magnetization relaxes to zero, traces of the original antiferromagnetic order are expected to show up in the long-time limit of two-point correlators $\sigma_j^z \sigma_{j+1}^z$ and $\sigma_j^x \sigma_{j+1}^x$. Our numerical result show that this is indeed the case.

As an alternative to the Néel state we could also choose the initial states

$$|\Psi_0\rangle_{\pm} = \frac{1}{\sqrt{2}}(|N\rangle \pm |AN\rangle),$$

where $|AN\rangle = |+-+-+-+\dots\rangle$ is the anti-Néel state. These states lead to correlation functions which are translationally invariant at all times. Moreover, the expectation values of the conserved charges are equal to the respective values in the Néel state, because in the infinite volume case considered here all cross-terms of the form $\langle N | Q_j | AN \rangle$ vanish. We note that the cross terms do not influence the time-dependent correlations either, because

$$\langle N | e^{iHt} \mathcal{O} e^{-iHt} | AN \rangle = 0 \quad (4.1)$$

at any finite t , given that \mathcal{O} is a localized operator and the infinite volume limit is already performed². Therefore the predictions of the same GGE hold in all three cases, but it is enough to calculate the conserved charges in $|N\rangle$.

The Néel state is not an eigenstate of the Hamiltonian, therefore the transfer matrix itself can not be used to calculate the mean values directly and the explicit form of the Q_j is required.

4.1 Conserved charges in the Néel state

Higher conserved charges of XXX and XYZ spin chains were considered in the papers [30, 31]. The basic tool of these papers is the boost operator [55, 56] given (in the XXZ case) by the formal expression

$$B = \sum_{j=-\infty}^{\infty} j(\sigma_j^x \sigma_{j+1}^x + \sigma_j^y \sigma_{j+1}^y + \Delta \sigma_j^z \sigma_{j+1}^z).$$

²In finite volume there are non-zero contributions to (4.1) when the t is large enough so that quasiparticles can travel around the volume and therefore a complete shift of the two states is possible.

It can be shown that the boost operator generates the derivative of the transfer matrix with respect to the spectral parameter:

$$[B, T(u)] \sim \dot{T}(u). \quad (4.2)$$

It follows that conserved charges are generated recursively as

$$[B, Q_j] \sim Q_{j+1}.$$

The equation above is to be understood up to additive constants.

The authors of [30, 31] considered the action of the commutator (4.3) and derived a recursive procedure to obtain all terms of the charges. They were able to analytically solve the recursion in the XXX case, whereas in the general XYZ case (including the XXZ chains) they derived the explicit form of the charges up to Q_6 .

In order to translate the results of [30, 31] into our conventions we define operators Q_j^{GM} as

$$\frac{1}{2}[B, Q_j^{\text{GM}}] = Q_{j+1}^{\text{GM}} \quad (4.3)$$

with the first member being

$$Q_2^{\text{GM}} = \sum_{j=-\infty}^{\infty} (\sigma_j^x \sigma_{j+1}^x + \sigma_j^y \sigma_{j+1}^y + \Delta \sigma_j^z \sigma_{j+1}^z).$$

Up to overall phase factors these operators coincide with the ones given in [30, 31] and they differ from the Q_j used in the present work in additive and multiplicative normalization. The additive constants can be fixed by requiring that all mean values vanish in the reference state $|F\rangle$; this follows from the fact that in our normalization

$$\langle F | \tau(u) | F \rangle = 1.$$

The multiplicative normalization can be deduced by working out the proof of (4.2) presented in [31] using our normalizations. We find the relation

$$Q_j = \frac{Q_j^{\text{GM}} - \langle F | Q_j^{\text{GM}} | F \rangle}{2(\sinh \eta)^{j-1}}. \quad (4.4)$$

An important basic result of [31] for the XYZ chain is that each conserved charge Q_j is a sum of terms of the form

$$[(\dots (\hat{\sigma}_{i_1} \times \tilde{\sigma}_{i_2}) \times \tilde{\sigma}_{i_3}) \dots \times \tilde{\sigma}_{i_{l-1}}] \cdot \hat{\sigma}_{i_l}. \quad (4.5)$$

Here (i_1, i_2, \dots, i_l) is a sequence of sites in increasing order such that $l \leq j$ and $i_l - i_1 < j$. The notation $\hat{\sigma}$ and $\tilde{\sigma}$ refers to vectors constructed out of rescaled Pauli-matrices. In the XXZ case they are

$$\hat{\sigma} = (\sigma^x, \sigma^y, \sqrt{\Delta} \sigma_z) \quad \tilde{\sigma} = (\sqrt{\Delta} \sigma^x, \sqrt{\Delta} \sigma^y, \sigma^z).$$

In the Néel state only those terms are non-vanishing which only include σ_z operators. From all possible terms in (4.5) we find such products only when $l = 2$, because any cross-product would necessarily involve at least one σ_x or σ_y operator. Therefore it is enough to collect the terms of the form $\sigma_i^z \sigma_{i+l}^z$. These terms only appear in the even charges Q_{2j} , which is consistent with the general statement that the mean values of the odd charges vanish in any parity invariant state.

The paper [31] provides formulas up to Q_6 . In order to obtain explicit representations for the higher charges we implemented the iteration procedure (4.3) with the symbolic manipulation program **form** [57]. The formal commutation relation (4.3) is only valid on an infinite spin chain, but it can still be used to calculate the charges. Defining the finite size operators

$$B^l = \sum_{j=1}^{l-1} j(\sigma_j^x \sigma_{j+1}^x + \sigma_j^y \sigma_{j+1}^y + \Delta \sigma_j^z \sigma_{j+1}^z)$$

$$Q_2^l = (\sigma_l^x \sigma_1^x + \sigma_l^y \sigma_1^y + \Delta \sigma_l^z \sigma_1^z) + \sum_{j=1}^{l-1} (\sigma_j^x \sigma_{j+1}^x + \sigma_j^y \sigma_{j+1}^y + \Delta \sigma_j^z \sigma_{j+1}^z)$$

we implemented the recursion

$$\frac{1}{2}[B^l, Q_j^l] = Q_{j+1}^l. \quad (4.6)$$

At each step of the iteration additional boundary terms arise which start to propagate towards the middle of the chain. However, if l is large enough then the "bulk" of Q_j^l is not affected and the coefficients of the different terms of Q_j^{GM} can be read off from the middle of the chain. We used this method to obtain all charges up to Q_{12} . For the sake of brevity we only present the terms relevant for the Néel state, and only up to Q_8 :

$$\begin{aligned}
Q_2^{\text{GM}} &= \sum_j \Delta \sigma_j^z \sigma_{j+1}^z + \dots \\
Q_4^{\text{GM}} &= \sum_j 4\Delta \sigma_j^z \sigma_{j+1}^z - 2\Delta \sigma_j^z \sigma_{j+2}^z + \dots \\
Q_6^{\text{GM}} &= \sum_j (56\Delta + 16\Delta^3) \sigma_j^z \sigma_{j+1}^z - (64\Delta + 8\Delta^3) \sigma_j^z \sigma_{j+2}^z + 24\Delta \sigma_j^z \sigma_{j+3}^z + \dots \\
Q_8^{\text{GM}} &= \sum_j (1504\Delta + 1312\Delta^3 + 64\Delta^5) \sigma_j^z \sigma_{j+1}^z - (2912\Delta + 1376\Delta^3 + 32\Delta^5) \sigma_j^z \sigma_{j+2}^z + \\
&\quad + (2400\Delta + 480\Delta^3) \sigma_j^z \sigma_{j+3}^z - 720\Delta \sigma_j^z \sigma_{j+4}^z + \dots
\end{aligned} \tag{4.7}$$

The dots represent terms with at least two σ^x or σ^y operators.

The Néel state mean values read (up to Q_{12})

$$\begin{aligned}
Q_2^N &= -2\Delta \\
Q_4^N &= -8\Delta \\
Q_6^N &= -(160\Delta + 32\Delta^3) \\
Q_8^N &= -(7808\Delta + 3584\Delta^3 + 128\Delta^5) \\
Q_{10}^N &= -(709120\Delta + 517632\Delta^3 + 62976\Delta^5 + 512\Delta^7) \\
Q_{12}^N &= -(103467008\Delta + 103763968\Delta^3 + 23973888\Delta^5 + 1036288\Delta^7 + 2048\Delta^9),
\end{aligned} \tag{4.8}$$

where we defined $Q_j^N = (\langle N | Q_j^{\text{GM}} | N \rangle - \langle F | Q_j^{\text{GM}} | F \rangle) / L$.

For the sake of completeness we also present the ferromagnetic expectation values of Q_j^{GM} . Defining $Q_j^F = \langle F | Q_j^{\text{GM}} | F \rangle / L$ we obtain

$$\begin{aligned}
Q_2^F &= \Delta \\
Q_4^F &= 2\Delta \\
Q_6^F &= 16\Delta + 8\Delta^3 \\
Q_8^F &= 272\Delta + 416\Delta^3 + 32\Delta^5 \\
Q_{10}^F &= 7936\Delta + 24576\Delta^3 + 7680\Delta^5 + 128\Delta^7 \\
Q_{12}^F &= 353792\Delta + 1841152\Delta^3 + 1304832\Delta^5 + 128512\Delta^7 + 512\Delta^9.
\end{aligned} \tag{4.9}$$

We stress that eqs. (4.9) represent the constant terms entering the r.h.s. of (4.4). The ferromagnetic eigenvalues of the higher charges all vanish in our normalization.

5 Numerical implementation

For our numerical calculations we considered the regime $\Delta > 1$. In this regime the XXZ chain is gapped: there are two ground states which become degenerate in the $L \rightarrow \infty$ limit, but there exists a finite gap between them and the next excited state. In the limit of $\Delta \rightarrow \infty$ the Hamiltonian turns into the classical Ising model, with its two ground states given by the Néel and anti-Néel states. Therefore quenching to a large but finite Δ can be considered a "small quench": we expect that all physical quantities predicted by the GGE will be close to their respective values in the Néel state. Departure from these mean values should show up for smaller Δ . For our actual numerical calculations we chose the values $\Delta = 2, 3, 4, 5$.

We implemented the NLIE (3.18) and solved it numerically by simple iteration, which converged even when the higher charges were added. It is known that the iteration method becomes ineffective in the low-temperature regime, where $\beta_2 \Delta$ is large. In this case a different formulation of the NLIE can be set up [34]; however this was not needed for our purposes.

We also implemented the factorized formulas of [53] for the short-range correlators

$$\langle \sigma_1^a \sigma_2^a \rangle, \langle \sigma_1^a \sigma_3^a \rangle \text{ and } \langle \sigma_1^a \sigma_4^a \rangle$$

for $a = z, x$. We checked our programs by calculating these correlators in the purely thermal case and comparing them to the values published in [37] and we found complete agreement.

We tested our numerics for the higher conserved charges by evaluating them in the purely thermal case and at low temperatures ($\beta_j = 0$ for $j > 3$ and $\beta_2 \rightarrow \infty$). In this limit the thermal averages quickly approach the eigenvalues in the two ground states, because the Hamiltonian is gapped. On the other hand, the ground state mean values can be found by standard Bethe Ansatz calculations [25]:

$$\lim_{\beta_2 \rightarrow \infty} \langle Q_{2j} \rangle = - \sum_{n=-\infty}^{\infty} (2n)^{2(j-1)} \frac{e^{-\eta|n|}}{\cosh(\eta n)}. \quad (5.1)$$

We compared our numerical results with the formula above and found convincing agreement. Note that the $\Delta \rightarrow \infty$ limit of (5.1) reproduces the leading terms of (4.8), given that the normalization (4.4) is used. This is a consequence of the fact that the states $(|N\rangle \pm |AN\rangle)/\sqrt{2}$ become the two ground states in the $\Delta \rightarrow \infty$ limit.

As a further numerical verification we also evaluated the high-temperature limit of the mean values. At high-temperatures any product of spin operators tends to zero, because the Pauli matrices are traceless operators. Therefore only the constant terms of Q_{2j} contribute and from (4.4) we obtain

$$\lim_{\beta_2 \rightarrow 0} \langle Q_{2j} \rangle = - \frac{\langle F | Q_{2j}^{\text{GM}} | F \rangle}{2(\sinh \eta)^{2j-1}}.$$

We compared our numerical results to those calculated from (4.9) and found complete agreement³.

In order to find the numerical values of the Lagrange multipliers $\beta_j^{(k)}$ we used the multi-dimensional Newton-Raphson method⁴. The matrix elements of the Jacobian

$$\frac{\partial \langle Q_m \rangle}{\partial \beta_n}$$

are easily obtained by taking a further derivative of (3.24). The Newton-Raphson method converged if started from a purely thermal state with an appropriate β_2 .

We observed that the numerics became sensitive to the choice of the integration contour for the NLIE as we add the higher charges. There are always two numbers $0 < \alpha_1$ and $\alpha_2 < \eta/2$ such that every α chosen from the interval $[\alpha_1, \alpha_2]$ gives the same answer for all quantities up to a desired numerical accuracy. However, the available interval for α shrinks with the growing number of the charges. This can be explained by the fact that the higher source terms for the NLIE are more and more singular, which in turn requires that the integration contour is far enough from the origin in order for the calculations to be stable. As a rule of thumb we used the values $\alpha = 0.95 \times \eta/2$.

In order to gather information about the Bethe roots of the QTM we calculated the function $L(\lambda) = (1 + \alpha(\lambda))$ along the imaginary axis using (3.18). Zeroes of $L(\lambda)$ determine the positions of the roots, which are known to be purely imaginary in the thermal case (at zero magnetic field). In all our examples it was found that although the position of the roots changes considerably as compared to the thermal case, they always stay on the imaginary axis. This provides a strong justification for the validity of the NLIE (3.18).

Having convinced ourselves that our numerics is stable, we computed the predictions for the short-range correlators. Our calculations were carried out with a total of $n = 400$ discretization points. When α was chosen from the stability interval, then the numerical values did not change up to 6 digits when we increased n to 600, or when we slightly changed α . We conclude that the results presented below are accurate up to the last digit.

Tables 1 and 2 include our numerical results. The correlation functions are also plotted as a function of the truncation level in figures 1 and 2.

Regarding the Lagrange multipliers our data is not sufficient to determine whether they are convergent as a function of the truncation level. Note that convergence of the β_j themselves is not required by

³The high-temperature limit of $\langle Q_{2j} \rangle$ could be calculated also from (3.23)-(3.24) using $\lim_{\beta_2 \rightarrow 0} \alpha(\lambda) = 1$.

⁴This was suggested by Gábor Takács.

physical principles, because they can not be measured. In fact higher charges can modify the lower β_j considerably, because they involve terms which are already present in the lower charges. We also calculated the cumulated coefficients γ_1 and γ_2 defined as

$$-\sum_{l=2}^k \beta_l^{(k)} Q_l = -\gamma_1 \sum_j \sigma_j^z \sigma_{j+1}^z - \gamma_2 \sum_j \sigma_j^z \sigma_{j+2}^z + \dots$$

Our results at $\Delta = 5$ are below:

| k | 2 | 4 | 6 | 8 | 10 | 12 |
|------------|--------|---------|---------|---------|---------|---------|
| γ_1 | 19.462 | 18.632 | 20.264 | 20.108 | 20.793 | 20.774 |
| γ_2 | 0 | 0.23873 | 0.22747 | 0.28444 | 0.28171 | 0.30213 |

These data are not sufficient to determine whether γ_1 and γ_2 are convergent.

Regarding the correlators we observe the following:

- For all Δ and all distances the $z - z$ correlators increase, the $x - x$ correlators decrease as a function of the truncation level. The physical reason for this is evident: The Néel state has maximal $z - z$ (anti-)correlations and identically zero $x - x$ correlations. Addition of higher conserved charges should reproduce more details of the initial state, leading to the observed behavior.
- All correlators seem to converge for $\Delta = 4$ and $\Delta = 5$. In order to convince ourselves we plotted the differences between the predictions at truncation level k and $k + 2$ on a log-scale. Fig. 3 (a) shows the change of $\langle \sigma_1^z \sigma_2^z \rangle$. Apart from a cycle with period 2 (which is a peculiarity of the Néel state, see below) we clearly see the exponential decay of the differences. Fig. 3 (b) shows the changes of $\langle \sigma_1^x \sigma_3^x \rangle$. Here we see the same behavior with approximately the same exponent, except for the points at $k = 2$. The fact that the truncated GGE predictions at $k = 2$ do not fit the exponential decay is not surprising: it is expected that for local operators spanning j sites the first j charges need to be added to reach the GGE prediction or at least the region where exponential convergence sets in. Similar behaviour was observed in the Ising chain in [13].
- At $\Delta = 2$ and $\Delta = 3$ the numerical data does not show convergence in the regime $k \leq 12$. In fact, plotting the differences on a log scale as before results in seemingly random data (Figs. 3 (c) and (d)). The correlations are monotonic functions of k and they are bounded so eventually they have to converge. We conjecture that there is exponential convergence also for $\Delta = 2$ and $\Delta = 3$, but it starts at some $k = k_c$ with $k_c > 12$.
- For large Δ all GGE predictions are close to the Néel values, where the $z - z$ correlations are maximal and the $x - x$ correlations are zero. For smaller Δ we see gradual departure towards the isotropic limit.

Summarizing the above findings the following picture emerges. There exists a “convergence length” κ which depends on Δ , such that for *every* short-range correlator \mathcal{O}

$$\langle \mathcal{O} \rangle^{(k)} = \langle \mathcal{O} \rangle_{GGE} + \left(\alpha + \beta(-1)^{k/2} \right) e^{-k/\kappa} + \dots, \text{ for } k > k_c, \quad (5.2)$$

where α, β and k_c depend of \mathcal{O} , and if \mathcal{O} spans at most j sites then $k_c \geq j$. The convergence length is small when the pre-quench and post-quench Hamiltonian are “close”, in our case when Δ is large. The dots on the r.h.s. of (5.2) denote contributions which decay faster than the leading correction. The form of (5.2) takes into account the observed oscillation with period 2, which is a peculiarity of the Néel state.

Due to the limitations of our data we do not perform any $k \rightarrow \infty$ fits of the correlators. For any practical purposes we suggest to take the values at $k = 12$. For larger Δ these data are already quite accurate, whereas for smaller Δ they are to be understood as lower or upper bounds, depending on the correlator in question. All our data shows clear difference between the thermal prediction ($k = 2$) and the approximation of the full GGE ($k = 12$). The differences are more pronounced for the 3-site and 4-site correlators.

We conclude this section by providing a possible explanation for the observed cycle of period 2 in Fig 3 (a) and (b). For any even k the charge Q_k has terms proportional to $(\sigma_j^z \sigma_{j+m}^z - 1)$ with $m = 1 \dots k/2$ [31], where we already subtracted the ferromagnetic expectation value. In the Néel state these terms evaluate to $(-1)^m - 1$; they vanish for every even m . Therefore, whenever $k = 4m$, the last two-site $z - z$ operator added to the GGE does not feel the antiferromagnetic order of the Néel state, in contrast to the charges $k = 4m + 2$ which are the ones who “submit” this information. This also explains the peculiar behavior of the thermal multiplier $\beta_2^{(k)}$: its value changes considerably when a new charge with $k = 4m + 2$ is added, but it almost stays the same when the truncation level is raised to $k = 4m + 4$.

6 Conclusions

We considered global quantum quenches in the XXZ spin chain and showed that the Generalized Gibbs Ensemble can be implemented within the Quantum Transfer Matrix framework, and it yields predictions for the long-time limit of short-range correlators. The central idea was to construct truncated GGE's with only a finite number of higher charges; we then investigated the convergence of the predictions as the truncation level is increased.

In our example we considered a quantum quench starting from the Néel state. Quenching to a finite but large Δ we found that our iterative procedure converges exponentially fast as a function of the truncation level. On the other hand, for smaller Δ convergence was not yet reached in the truncated GGE's with the first 12 charges.

Correlations in the long-time limit are close to their values in the Néel state when we quench to a large Δ . On the other hand, quenching to smaller Δ the system departs towards the isotropic correlations. An important result of the present work is that the addition of the higher charges forces the correlations towards their Néel values. This is consistent with the general idea behind GGE, namely that the existence of the higher charges constrains the dynamics and physical observables can not relax to their thermal values.

One of our original expectations was to find that adding k charges to the GGE would fix all correlators spanning at most k sites, possibly with negligible correction terms. Our findings show that this is only true, when the pre-quench and post-quench Hamiltonians are sufficiently close. Furthermore, even in these cases the dependence on the truncation level looks very similar for all correlators (see fig. 1). In our case we found that the x-x correlations reveal the expected pattern: exponential decay of the corrections sets in when the required number of higher charges is already added (compare figs. 3(a) and 3(b)).

Our results show that the convergence length κ (governing the convergence as we add the higher charges) is small for “small quenches” and that it is a new length scale which is independent of the correlation lengths of the system. It is an interesting question how κ depends on the pre-quench and post-quench Hamiltonians in more general situations.

It would be interesting to consider the quench from the Néel state at the isotropic point ($\Delta = 1$). Although this particular case is expected to exhibit the slowest convergence as a function of the truncation level, one advantage would be that in the XXX case all terms in the higher charges are known analytically [30], therefore it might be possible to reach much higher truncation levels.

The present methods could be applied to other quench situations as well. The only requirement is that the mean values of the conserved charges in the initial state should be evaluated exactly. In principle this is possible even for a finite interaction quench $\Delta \rightarrow \tilde{\Delta}$, because the charges of the post-quench Hamiltonian are nothing more than certain combinations of Pauli matrices, and their mean values in the pre-quench ground state could be obtained by already available techniques.

We would like to stress that in this work we did not attempt to prove the GGE hypothesis. Instead, our numerical results could be used as test of the GGE. We determined both the thermal and GGE predictions, and we expect that independent numerical investigations could confirm one of the two, or they could point to a different result. Numerical methods which simulate real-time dynamics typically involve a certain amount of integrability breaking, therefore they are expected to converge to our thermal predictions (the rows with $k = 2$ in the Tables 1 and 2), possibly with a pre-thermalization regime where the GGE applies.

Acknowledgments

We are grateful to Gábor Takács and Márton Kormos for stimulating discussions and useful comments on the manuscript. Also, we are indebted to Jean-Sébastien Caux for many discussions about related problems, which motivated us to study quench dynamics in XXZ chains.

References

- [1] M. Rigol, V. Dunjko, and M. Olshanii, “Thermalization and its mechanism for generic isolated quantum systems,” *Nature* **452** (2008) 854–858, [arXiv:0708.1324 \[cond-mat.stat-mech\]](https://arxiv.org/abs/0708.1324).

[2] A. Polkovnikov, K. Sengupta, A. Silva, and M. Vengalattore, “*Colloquium* : Nonequilibrium dynamics of closed interacting quantum systems,” *Rev. Mod. Phys.* **83** (2011) 863–883.

[3] M. Rigol, V. Dunjko, V. Yurovsky, and M. Olshanii, “Relaxation in a Completely Integrable Many-Body Quantum System: An Ab Initio Study of the Dynamics of the Highly Excited States of 1D Lattice Hard-Core Bosons,” *Phys. Rev. Lett.* **98** (2007) no. 5, 050405, [arXiv:cond-mat/0604476](https://arxiv.org/abs/0604476).

[4] J.-S. Caux and F. H. L. Essler, “Time evolution of local observables after quenching to an integrable model,” *ArXiv e-prints* (2013) , [arXiv:1301.3806](https://arxiv.org/abs/1301.3806) [cond-mat.stat-mech].

[5] P. Barmettler, M. Punk, V. Gritsev, E. Demler, and E. Altman, “Quantum quenches in the anisotropic spin-1/2 Heisenberg chain: different approaches to many-body dynamics far from equilibrium,” *New Journal of Physics* **12** (2010) no. 5, 055017, [arXiv:0911.1927](https://arxiv.org/abs/0911.1927) [cond-mat.quant-gas].

[6] D. Rossini, A. Silva, G. Mussardo, and G. E. Santoro, “Effective Thermal Dynamics Following a Quantum Quench in a Spin Chain,” *Physical Review Letters* **102** (2009) no. 12, 127204, [arXiv:0810.5508](https://arxiv.org/abs/0810.5508) [cond-mat.stat-mech].

[7] D. Rossini, S. Suzuki, G. Mussardo, G. E. Santoro, and A. Silva, “Long time dynamics following a quench in an integrable quantum spin chain: Local versus nonlocal operators and effective thermal behavior,” *Phys. Rev. B* **82** (2010) no. 14, 144302, [arXiv:1002.2842](https://arxiv.org/abs/1002.2842) [cond-mat.stat-mech].

[8] P. Calabrese, F. H. L. Essler, and M. Fagotti, “Quantum quench in the transverse field Ising chain: I. Time evolution of order parameter correlators,” *Journal of Statistical Mechanics: Theory and Experiment* **7** (2012) 16, [arXiv:1204.3911](https://arxiv.org/abs/1204.3911) [cond-mat.quant-gas].

[9] P. Calabrese, F. H. L. Essler, and M. Fagotti, “Quantum quenches in the transverse field Ising chain: II. Stationary state properties,” *Journal of Statistical Mechanics: Theory and Experiment* **7** (2012) 22, [arXiv:1205.2211](https://arxiv.org/abs/1205.2211) [cond-mat.stat-mech].

[10] B. Blass, H. Rieger, and F. Iglói, “Quantum relaxation and finite-size effects in the XY chain in a transverse field after global quenches,” *EPL (Europhysics Letters)* **99** (2012) 30004, [arXiv:1205.3303](https://arxiv.org/abs/1205.3303) [cond-mat.stat-mech].

[11] F. H. L. Essler, S. Evangelisti, and M. Fagotti, “Dynamical Correlations After a Quantum Quench,” *Physical Review Letters* **109** (2012) no. 24, 247206, [arXiv:1208.1961](https://arxiv.org/abs/1208.1961) [cond-mat.stat-mech].

[12] T. Caneva, E. Canovi, D. Rossini, G. E. Santoro, and A. Silva, “Applicability of the generalized Gibbs ensemble after a quench in the quantum Ising chain,” *Journal of Statistical Mechanics: Theory and Experiment* **7** (2011) 15, [arXiv:1105.3176](https://arxiv.org/abs/1105.3176) [cond-mat.stat-mech].

[13] M. Fagotti and F. H. L. Essler, “Reduced Density Matrix after a Quantum Quench,” *ArXiv e-prints* (2013) , [arXiv:1302.6944](https://arxiv.org/abs/1302.6944) [cond-mat.stat-mech].

[14] P. Calabrese and J. Cardy, “Quantum quenches in extended systems,” *Journal of Statistical Mechanics: Theory and Experiment* **2007** (2007) no. 06, P06008, [arXiv:0704.1880](https://arxiv.org/abs/0704.1880) [cond-mat.stat-mech].

[15] A. C. Cassidy, C. W. Clark, and M. Rigol, “Generalized Thermalization in an Integrable Lattice System,” *Physical Review Letters* **106** (2011) no. 14, 140405, [arXiv:1008.4794](https://arxiv.org/abs/1008.4794) [cond-mat.stat-mech].

[16] V. Gurarie, “Global large time dynamics and the generalized Gibbs ensemble,” *Journal of Statistical Mechanics: Theory and Experiment* **2** (2013) 14, [arXiv:1209.3816](https://arxiv.org/abs/1209.3816) [cond-mat.stat-mech].

[17] J. M. Zhang, F. C. Cui, and J. Hu, “Dynamical predictive power of the generalized Gibbs ensemble revealed in a second quench,” *Phys. Rev. E* **85** (2012) 041138.

[18] T. Barthel and U. Schollwöck, “Dephasing and the Steady State in Quantum Many-Particle Systems,” *Physical Review Letters* **100** (2008) no. 10, 100601, [arXiv:0711.4896](https://arxiv.org/abs/0711.4896) [cond-mat.stat-mech].

[19] M. Kollar and M. Eckstein, “Relaxation of a one-dimensional Mott insulator after an interaction quench,” *Phys. Rev. A* **78** (2008) no. 1, 013626, [arXiv:0804.2254](https://arxiv.org/abs/0804.2254) [cond-mat.str-el].

[20] M. A. Cazalilla, A. Iucci, and M.-C. Chung, “Thermalization and quantum correlations in exactly solvable models,” *Phys. Rev. E* **85** (2012) no. 1, 011133, [arXiv:1106.5206](https://arxiv.org/abs/1106.5206) [cond-mat.stat-mech].

[21] A. Iucci and M. A. Cazalilla, “Quantum quench dynamics of the Luttinger model,” *Phys. Rev. A* **80** (2009) no. 6, 063619, [arXiv:0903.1205](https://arxiv.org/abs/0903.1205) [cond-mat.str-el].

[22] J.-S. Caux and R. M. Konik, “Numerical renormalization based on integrable theories: quantum quenches and their corresponding generalized Gibbs ensembles,” *ArXiv e-prints* (2012) , [arXiv:1203.0901](https://arxiv.org/abs/1203.0901) [cond-mat.quant-gas].

[23] J. Mossel and J.-S. Caux, “Generalized TBA and generalized Gibbs,” *Journal of Physics A Mathematical General* **45** (2012) no. 25, 255001, [arXiv:1203.1305](https://arxiv.org/abs/1203.1305) [cond-mat.quant-gas].

[24] C. N. Yang and C. P. Yang, “Thermodynamics of a One-Dimensional System of Bosons with Repulsive Delta-Function Interaction,” *J. Math. Phys.* **10** (1969) 1115.

[25] M. Takahashi, *Thermodynamics of One-Dimensional Solvable Models*. Cambridge University Press, 1999.

[26] D. Fioretto and G. Mussardo, “Quantum Quenches in Integrable Field Theories,” *New Journal of Physics* **12** (2009) 055015, [arxiv:0911.3345](https://arxiv.org/abs/0911.3345) [cond-mat.stat-mech].

[27] B. Pozsgay, “Mean values of local operators in highly excited Bethe states,” *J. Stat. Mech.* **2011** (2011) P01011, [arXiv:1009.4662](https://arxiv.org/abs/1009.4662) [hep-th].

[28] M. Kormos, Y.-Z. Chou, and A. Imambekov, “Exact three-body local correlations for excited states of the 1D Bose gas,” *ArXiv e-prints* (July, 2011) , [arXiv:1108.0145](https://arxiv.org/abs/1108.0145) [cond-mat.quant-gas].

[29] B. Davies and V. E. Korepin, “Higher conservation laws for the quantum non-linear Schroedinger equation,” *ArXiv e-prints* (2011) , [arXiv:1109.6604](https://arxiv.org/abs/1109.6604) [math-ph].

[30] M. P. Grabowski and P. Mathieu, “Quantum integrals of motion for the Heisenberg spin chain,” *Mod.Phys.Lett.* **A9** (1994) 2197–2206, [arXiv:hep-th/9403149](https://arxiv.org/abs/hep-th/9403149) [hep-th].

[31] M. Grabowski and P. Mathieu, “Structure of the conservation laws in integrable spin chains with short range interactions,” *Annals Phys.* **243** (1995) 299–371, [arXiv:hep-th/9411045](https://arxiv.org/abs/hep-th/9411045) [hep-th].

[32] A. Klauser and J.-S. Caux, “Equilibrium thermodynamic properties of interacting two-component bosons in one dimension,” *Phys. Rev. A* **84** (2011) no. 3, 033604, [arXiv:1106.4971](https://arxiv.org/abs/1106.4971) [cond-mat.quant-gas].

[33] A. Klümper, “Thermodynamics of the anisotropic spin-1/2 Heisenberg chain and related quantum chains,” *Zeitschrift für Physik B Condensed Matter* **91** (1993) 507–519.

[34] A. Klümper, “Integrability of Quantum Chains: Theory and Applications to the Spin-1/2 XXZ Chain,” in *Quantum Magnetism*, U. Schollwöck, J. Richter, D. J. J. Farnell, & R. F. Bishop , ed., vol. 645 of *Lecture Notes in Physics*, Berlin Springer Verlag, p. 349. 2004. [arXiv:cond-mat/0502431](https://arxiv.org/abs/cond-mat/0502431).

[35] M. Takahashi, M. Shiroishi, and A. Klümper, “Equivalence of TBA and QTM,” *J. Phys. A* **34** (2001) no. 13, L187.

[36] H. E. Boos, J. Damerau, F. Göhmann, A. Klümper, J. Suzuki, and A. Weiße, “Short-distance thermal correlations in the XXZ chain,” *Journal of Statistical Mechanics: Theory and Experiment* **8** (2008) 10, [arXiv:0806.3953](https://arxiv.org/abs/0806.3953) [cond-mat.str-el].

[37] C. Trippe, F. Göhmann, and A. Klümper, “Short-distance thermal correlations in the massive XXZ chain,” *European Physical Journal B* **73** (2010) 253–264, [arXiv:0908.2232](https://arxiv.org/abs/0908.2232) [cond-mat.str-el].

[38] J. Sato, B. Aufgebauer, H. Boos, F. Göhmann, A. Klümper, M. Takahashi, and C. Trippe, “Computation of static Heisenberg-chain correlators: Control over length and temperature dependence,” (2011) , [arXiv:1105.4447](https://arxiv.org/abs/1105.4447).

[39] A. Klümper and K. Sakai, “The thermal conductivity of the spin- 1/2 XXZ chain at arbitrary temperature,” *Journal of Physics A Mathematical General* **35** (2002) 2173–2182, [arXiv:cond-mat/0112444](https://arxiv.org/abs/cond-mat/0112444).

[40] K. Sakai and A. Klümper, “Non-dissipative thermal transport in the massive regimes of the XXZ chain,” *Journal of Physics A Mathematical General* **36** (2003) 11617–11629, [arXiv:cond-mat/0307227](https://arxiv.org/abs/cond-mat/0307227).

- [41] A. A. Zvyagin and A. Klümper, “Quantum phase transitions and thermodynamics of quantum antiferromagnets with next-nearest-neighbor couplings,” *Phys. Rev. B* **68** (2003) 144426.
- [42] C. Trippe and A. Klümper, “Quantum phase transitions and thermodynamics of quantum antiferromagnets with competing interactions,” *Low Temperature Physics* **33** (2007) 920–926, [arXiv:0709.0229 \[cond-mat.str-el\]](https://arxiv.org/abs/0709.0229).
- [43] P. Barmettler, M. Punk, V. Gritsev, E. Demler, and E. Altman, “Relaxation of Antiferromagnetic Order in Spin-1/2 Chains Following a Quantum Quench,” *Physical Review Letters* **102** (2009) no. 13, 130603, [arXiv:0810.4845 \[cond-mat.other\]](https://arxiv.org/abs/0810.4845).
- [44] H. Bethe, “Zur Theorie der Metalle,” *Zeitschrift für Physik* **A71** (1931) 205.
- [45] R. Orbach, “Linear Antiferromagnetic Chain with Anisotropic Coupling,” *Phys. Rev.* **112** (1958) no. 2, 309–316.
- [46] L. R. Walker, “Antiferromagnetic Linear Chain,” *Phys. Rev.* **116** (1959) no. 5, 1089–1090.
- [47] C. N. Yang and C. P. Yang, “One-Dimensional Chain of Anisotropic Spin-Spin Interactions. I. Proof of Bethe’s Hypothesis for Ground State in a Finite System,” *Phys. Rev.* **150** (1966) no. 1, 321–327.
- [48] C. N. Yang, “Some Exact Results for the Many-Body Problem in one Dimension with Repulsive Delta-Function Interaction,” *Phys. Rev. Lett.* **19** (1967) 1312–1315.
- [49] R. J. Baxter, *Exactly solved models in statistical mechanics*. London: Academic Press Inc, 1982.
- [50] M. Lüscher, “Dynamical charges in the quantized renormalized massive Thirring model,” *Nuclear Physics B* **117** (1976) no. 2, 475 – 492.
- [51] V. Korepin, N. Bogoliubov, and A. Izergin, *Quantum inverse scattering method and correlation functions*. Cambridge University Press, 1993.
- [52] F. Göhmann, A. Klümper, and A. Seel, “Integral representations for correlation functions of the XXZ chain at finite temperature,” *Journal of Physics A Mathematical General* **37** (2004) 7625–7651, [arXiv:hep-th/0405089](https://arxiv.org/abs/hep-th/0405089).
- [53] H. E. Boos, F. Göhmann, A. Klümper, and J. Suzuki, “Factorization of the finite temperature correlation functions of the XXZ chain in a magnetic field,” *J. Phys. A* **40** (2007) 10699, [arXiv:0705.2716](https://arxiv.org/abs/0705.2716).
- [54] H. Boos, M. Jimbo, T. Miwa, F. Smirnov, and Y. Takeyama, “Algebraic Representation of Correlation Functions in Integrable Spin Chains,” *Annales Henri Poincaré* **7** (2006) 1395–1428, [arXiv:hep-th/0601132](https://arxiv.org/abs/hep-th/0601132).
- [55] M. G. Tetelman *Sovj. Phys. JETP* **1981** (55) 306.
- [56] H. B. Thacker, “Corner transfer matrices and Lorentz invariance on a lattice,” *Physica D Nonlinear Phenomena* **18** (1986) 348–359.
- [57] J. A. M. Vermaasen, “New features of FORM,” *ArXiv Mathematical Physics e-prints* (2000) , [arXiv:math-ph/0010025](https://arxiv.org/abs/math-ph/0010025).

| k | $\beta_2^{(k)}$ | $\beta_4^{(k)}$ | $\beta_6^{(k)}$ | $\beta_8^{(k)}$ | $\beta_{10}^{(k)}$ | $\beta_{12}^{(k)}$ |
|-----|-----------------|----------------------------|---------------------------|----------------------------|---------------------------|----------------------------|
| 2 | 1.425983 | | | | | |
| 4 | 1.446665 | -1.645590×10^{-2} | | | | |
| 6 | 1.809022 | -1.858076×10^{-1} | 9.534796×10^{-3} | | | |
| 8 | 1.856607 | -2.907996×10^{-1} | 1.606714×10^{-2} | -9.262052×10^{-5} | | |
| 10 | 2.058829 | -4.366422×10^{-1} | 3.261496×10^{-2} | -4.227379×10^{-4} | 1.792828×10^{-6} | |
| 12 | 2.084167 | -5.414107×10^{-1} | 4.392467×10^{-2} | -7.655830×10^{-4} | 4.745685×10^{-6} | -7.809887×10^{-9} |

| k | $\langle \sigma_1^z \sigma_2^z \rangle$ | $\langle \sigma_1^z \sigma_3^z \rangle$ | $\langle \sigma_1^z \sigma_4^z \rangle$ | $\langle \sigma_1^x \sigma_2^x \rangle$ | $\langle \sigma_1^x \sigma_3^x \rangle$ | $\langle \sigma_1^x \sigma_4^x \rangle$ |
|-----|---|---|---|---|---|---|
| 2 | -0.612933 | 0.337184 | -0.217441 | -0.387067 | 0.089492 | -0.036689 |
| 4 | -0.615407 | 0.340498 | -0.224563 | -0.384593 | 0.087323 | -0.037779 |
| 6 | -0.633311 | 0.364773 | -0.254495 | -0.366689 | 0.079573 | -0.026466 |
| 8 | -0.638963 | 0.372576 | -0.263839 | -0.361037 | 0.077668 | -0.023009 |
| 10 | -0.645892 | 0.382295 | -0.275347 | -0.354108 | 0.075581 | -0.018792 |
| 12 | -0.648906 | 0.386578 | -0.280383 | -0.351094 | 0.074730 | -0.016958 |

(a) $\Delta = 2$

| k | $\beta_2^{(k)}$ | $\beta_4^{(k)}$ | $\beta_6^{(k)}$ | $\beta_8^{(k)}$ | $\beta_{10}^{(k)}$ | $\beta_{12}^{(k)}$ |
|-----|-----------------|----------------------------|---------------------------|----------------------------|---------------------------|----------------------------|
| 2 | 2.509646 | | | | | |
| 4 | 2.579696 | -2.307552×10^{-1} | | | | |
| 6 | 3.001455 | -6.465130×10^{-1} | 4.852242×10^{-2} | | | |
| 8 | 3.000383 | -8.891678×10^{-1} | 7.641464×10^{-2} | -7.568640×10^{-4} | | |
| 10 | 3.172756 | -1.182961 | 1.392459×10^{-1} | -3.008985×10^{-3} | 2.183419×10^{-5} | |
| 12 | 3.173845 | -1.368100 | 1.759998×10^{-1} | -4.936284×10^{-3} | 5.064619×10^{-5} | -1.331293×10^{-7} |

| k | $\langle \sigma_1^z \sigma_2^z \rangle$ | $\langle \sigma_1^z \sigma_3^z \rangle$ | $\langle \sigma_1^z \sigma_4^z \rangle$ | $\langle \sigma_1^x \sigma_2^x \rangle$ | $\langle \sigma_1^x \sigma_3^x \rangle$ | $\langle \sigma_1^x \sigma_4^x \rangle$ |
|-----|---|---|---|---|---|---|
| 2 | -0.778391 | 0.585901 | -0.486765 | -0.332413 | 0.059452 | -0.024717 |
| 4 | -0.792940 | 0.612660 | -0.530385 | -0.310590 | 0.050655 | -0.024848 |
| 6 | -0.808696 | 0.640589 | -0.564324 | -0.286956 | 0.044700 | -0.010937 |
| 8 | -0.8115893 | 0.6456882 | -0.5704706 | -0.2826161 | 0.0437445 | -0.0084729 |
| 10 | -0.8136196 | 0.6492727 | -0.5747833 | -0.2795706 | 0.0431133 | -0.0067519 |
| 12 | -0.8140907 | 0.6501061 | -0.5757850 | -0.2788640 | 0.0429724 | -0.0063530 |

(b) $\Delta = 3$

Table 1: The Lagrange multipliers of the truncated GGE's and the predictions for the short-range correlators as a function of the truncation level.

| k | $\beta_2^{(k)}$ | $\beta_4^{(k)}$ | $\beta_6^{(k)}$ | $\beta_8^{(k)}$ | $\beta_{10}^{(k)}$ | $\beta_{12}^{(k)}$ |
|-----|-----------------|----------------------------|---------------------------|----------------------------|---------------------------|----------------------------|
| 2 | 3.324318 | | | | | |
| 4 | 3.311865 | -4.272592×10^{-1} | | | | |
| 6 | 3.680208 | -1.055429 | 1.010927×10^{-1} | | | |
| 8 | 3.670066 | -1.383075 | 1.524210×10^{-1} | -1.791012×10^{-3} | | |
| 10 | 3.821611 | -1.908843 | 2.914045×10^{-1} | -8.182288×10^{-3} | 7.859512×10^{-5} | |
| 12 | 3.822664 | -2.195990 | 3.660003×10^{-1} | -1.294490×10^{-2} | 1.682970×10^{-4} | -5.214364×10^{-7} |

| k | $\langle \sigma_1^z \sigma_2^z \rangle$ | $\langle \sigma_1^z \sigma_3^z \rangle$ | $\langle \sigma_1^z \sigma_4^z \rangle$ | $\langle \sigma_1^x \sigma_2^x \rangle$ | $\langle \sigma_1^x \sigma_3^x \rangle$ | $\langle \sigma_1^x \sigma_4^x \rangle$ |
|-----|---|---|---|---|---|---|
| 2 | -0.868150 | 0.745564 | -0.680444 | -0.263701 | 0.036000 | -0.013281 |
| 4 | -0.879100 | 0.766869 | -0.713671 | -0.241800 | 0.029953 | -0.012251 |
| 6 | -0.8861283 | 0.7800751 | -0.7298895 | -0.2277434 | 0.0273182 | -0.0044624 |
| 8 | -0.8868965 | 0.7815109 | -0.7316455 | -0.2262069 | 0.0270605 | -0.0036317 |
| 10 | -0.8873471 | 0.7823539 | -0.7326757 | -0.2253059 | 0.0269172 | -0.0031453 |
| 12 | -0.8874100 | 0.7824718 | -0.7328197 | -0.2251799 | 0.0268979 | -0.0030773 |

(a) $\Delta = 4$

| k | $\beta_2^{(k)}$ | $\beta_4^{(k)}$ | $\beta_6^{(k)}$ | $\beta_8^{(k)}$ | $\beta_{10}^{(k)}$ | $\beta_{12}^{(k)}$ |
|-----|-----------------|----------------------------|---------------------------|----------------------------|---------------------------|----------------------------|
| 2 | 3.892437 | | | | | |
| 4 | 3.821985 | -5.729564×10^{-1} | | | | |
| 6 | 4.164352 | -1.447134 | 1.638562×10^{-1} | | | |
| 8 | 4.156574 | -1.859024 | 2.415704×10^{-1} | -3.060743×10^{-3} | | |
| 10 | 4.298095 | -2.782744 | 5.102938×10^{-1} | -1.720161×10^{-2} | 1.965757×10^{-4} | |
| 12 | 4.299221 | -3.243448 | 6.472767×10^{-1} | -2.681533×10^{-2} | 4.010930×10^{-4} | -1.338719×10^{-6} |

| k | $\langle \sigma_1^z \sigma_2^z \rangle$ | $\langle \sigma_1^z \sigma_3^z \rangle$ | $\langle \sigma_1^z \sigma_4^z \rangle$ | $\langle \sigma_1^x \sigma_2^x \rangle$ | $\langle \sigma_1^x \sigma_3^x \rangle$ | $\langle \sigma_1^x \sigma_4^x \rangle$ |
|-----|---|---|---|---|---|---|
| 2 | -0.9151778 | 0.8340633 | -0.7910349 | -0.2120556 | 0.0229398 | -0.0072106 |
| 4 | -0.9217059 | 0.8469762 | -0.8108822 | -0.1957353 | 0.0194593 | -0.0064598 |
| 6 | -0.9248945 | 0.8531096 | -0.8184590 | -0.1877637 | 0.0182649 | -0.0021925 |
| 8 | -0.9251263 | 0.8535539 | -0.8190064 | -0.1871842 | 0.0181865 | -0.0018872 |
| 10 | -0.9252532 | 0.8537971 | -0.8193061 | -0.1868671 | 0.0181458 | -0.0017203 |
| 12 | -0.9252648 | 0.8538195 | -0.8193336 | -0.1868380 | 0.0181422 | -0.0017050 |

(b) $\Delta = 5$

Table 2: The Lagrange multipliers of the truncated GGE's and the predictions for the short-range correlators as a function of the truncation level

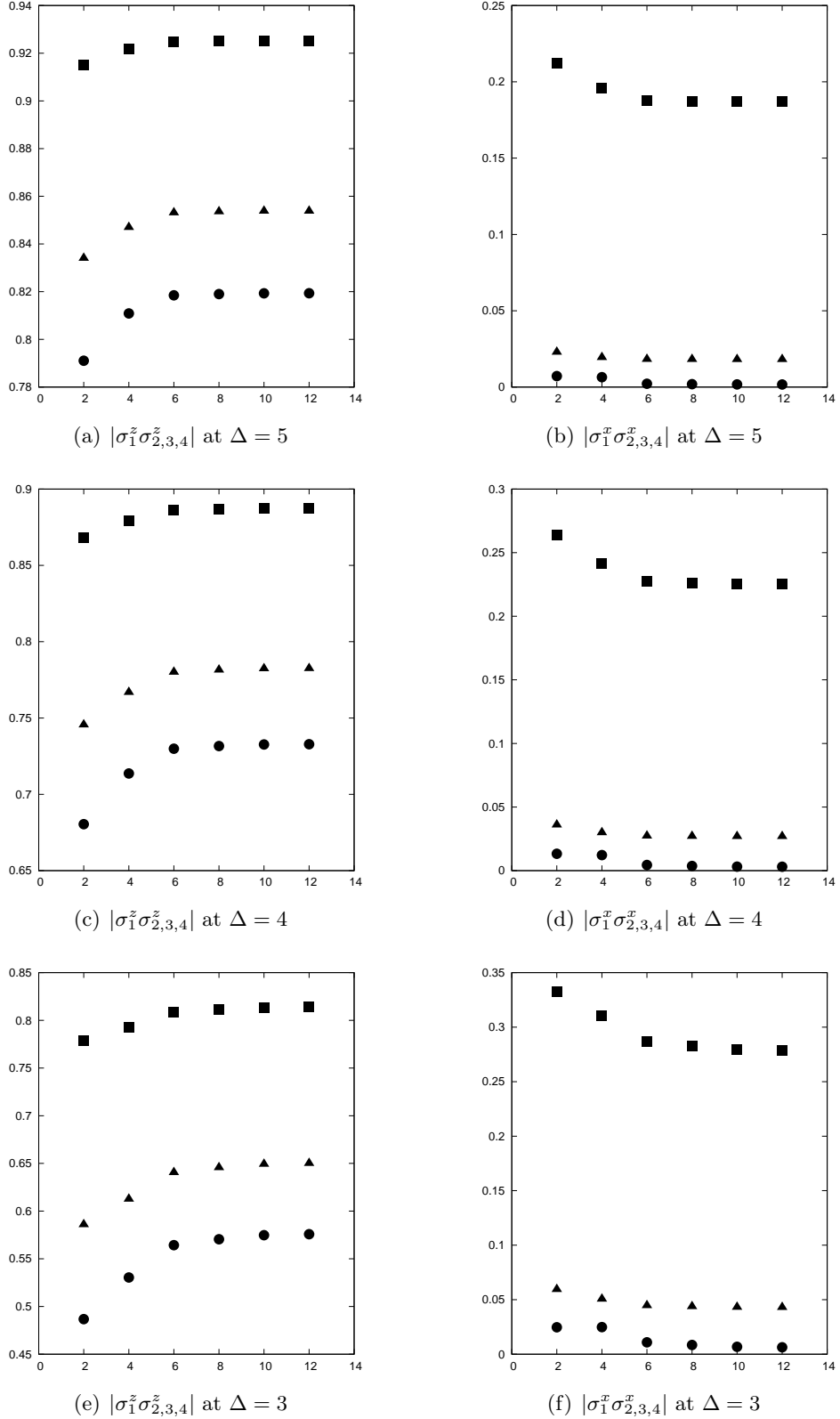
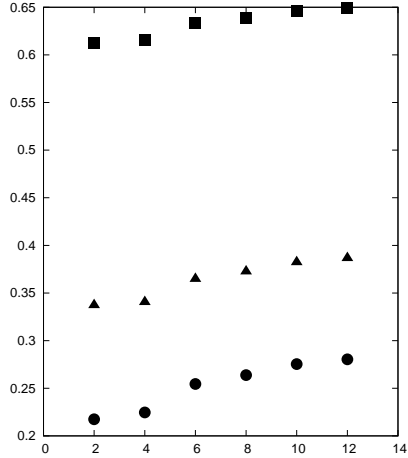
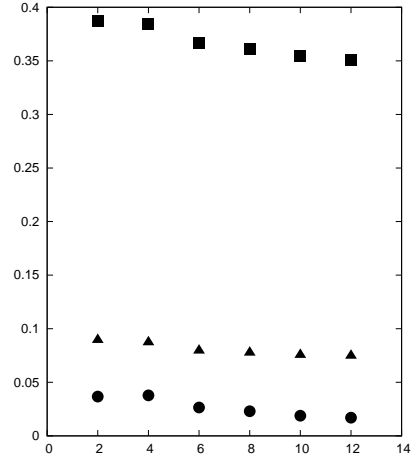


Figure 1: The short-range correlators predicted by the truncated GGE's as a function of the truncation level. The top, middle and bottom curves correspond to $\sigma_1^a \sigma_{1+j}^a$ with $j = 1, 2$, and 3 , respectively. We plotted the magnitude of the correlators, the signs are given by $(-1)^j$.

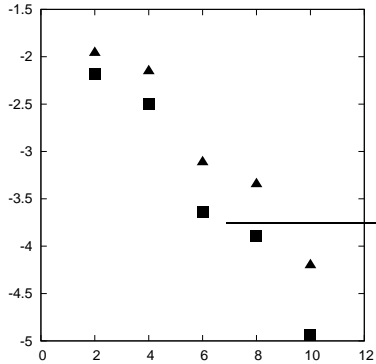


(a) $|\sigma_1^z \sigma_2^z,_{3,4}|$ at $\Delta = 2$

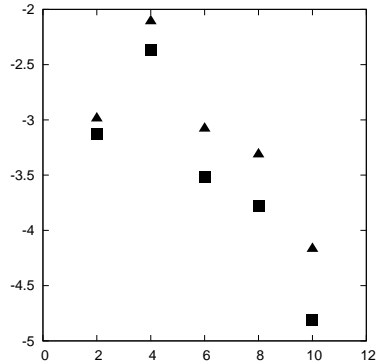


(b) $|\sigma_1^x \sigma_2^x,_{3,4}|$ at $\Delta = 2$

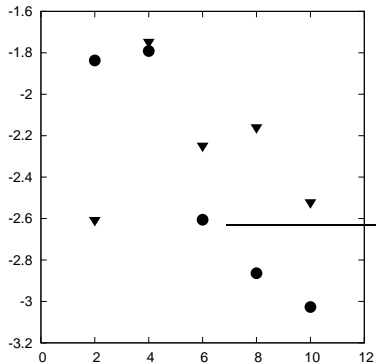
Figure 2: The short-range correlators predicted by the truncated GGE's as a function of the truncation level. The top, middle and bottom curves correspond to $\sigma_1^a \sigma_{1+j}^a$ with $j = 1, 2$, and 3 , respectively. We plotted the magnitude of the correlators, the signs are given by $(-1)^j$.



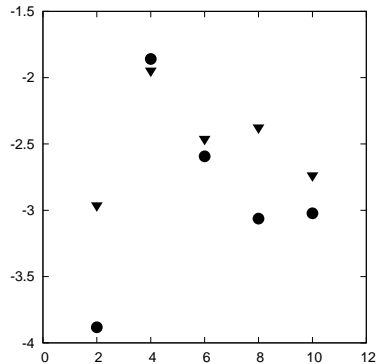
(a) $\mathcal{O} = \sigma_1^z \sigma_2^z$ for $\Delta = 4$ (triangles) and $\Delta = 5$ (squares)



(b) $\mathcal{O} = \sigma_1^x \sigma_2^x$ for $\Delta = 4$ (triangles) and $\Delta = 5$ (squares)



(c) $\mathcal{O} = \sigma_1^z \sigma_2^z$ for $\Delta = 2$ (triangles) and $\Delta = 3$ (squares)



(d) $\mathcal{O} = \sigma_1^x \sigma_2^x$ for $\Delta = 2$ (triangles) and $\Delta = 3$ (squares)

Figure 3: $\log(|\mathcal{O}^{(k+2)} - \mathcal{O}^{(k)}|)$ as a function of k .